Transportation Research Part C 86 (2018) 328–345

Contents lists available at ScienceDirect

Transportation Research Part C

journal homepage: www.elsevier.com/locate/trc

Integration of adaptive signal control and freeway off-ramp priority control for commuting corridors

Xianfeng Yang[a,*], Yao Cheng[b], Gang-Len Chang[b]

[a] Department of Civil and Environmental Engineering, University of Utah, United States
[b] Department of Civil & Environmental Engineering, University of Maryland, United States

ARTICLE INFO

Keywords:
Adaptive signal control
Off-ramp priority control
Green extension
Dynamic signal progression

ABSTRACT

Congestion at the downstream of an off-ramp often propagates the traffic queue to the freeway mainline, and thus reduces the freeway capacity at the interchange area. To prevent such potential queue spillover and improve traffic control efficiency over the entire corridor, this study develops an integrated control system which includes three primary functions: off-ramp queue estimation, arterial adaptive signal operations, and freeway off-ramp priority control. Using detected flow data, the system firstly estimates the queue length on the target off-ramp. If no potential queue spillover is predicted, the adaptive signal control function will then adjust the intersection signal timings and provide dynamic signal progression to critical path-flows. Otherwise, the off-ramp priority control function will be activated to clear the queuing vehicles at the off-ramp. To evaluate the effectiveness of the proposed system, this study has conducted numerical studies on a freeway interchange using a well-calibrated simulation platform. The experimental results reveal that the overall network performance can indeed be improved under the proposed control system, compared with other operational strategies. Further analyses of freeway time-dependent travel time distribution also evidence the effectiveness of the proposed system in preventing off-ramp queue spillover.

1. Introduction

Since the operational performance of freeway segment and its neighboring local streets are often mutually dependent, a large body of literature related to concurrent control of the freeway and local arterial has been reported over the past decades. Most of such studies, however, focused on the on-ramp metering controls and their coordinated operations (Pooran and Lieu, 1994; Tian et al., 2002; Lu et al., 2013). A comprehensive review of such studies can be found in the study by Papageorgiou and Kotsialos (2000).

In contrast, the equally critical issue of off-ramp control has not yet received adequate attentions. As described by Lovell (1997), most drivers tend to not segregate themselves by destination well in advance of an off-ramp, but rather make most of their lane-changing decisions at the last moment. The exit queue of an off-ramp might spread itself laterally upstream of an off-ramp, thereby restricting the efficiency of the mainline flow. Hence, congested conditions at downstream intersections can lead to a long traffic queue at the off-ramp. Consequently, the queue spillback may propagate to upstream and block freeway lanes (Daganzo et al., 1999; Muñoz and Daganzo, 2002; Jia et al., 2004). Considering a partial blockage of the right lane, Newell (1999) proposed a model to evaluate the delays on a freeway when queues from an exit ramp spill back to the freeway mainline. Cassidy et al. (2002) studied the exiting queue of an off-ramp using field data from video-tapes, and find that a bottleneck with a diminished capacity arises on a

* Corresponding author at: 110 Central Campus Dr. Room 2133, Salt Lake City, UT 84112, United States.
E-mail addresses: xyang@mail.sdsu.edu (X. Yang), gang@umd.edu (G.-L. Chang).

https://doi.org/10.1016/j.trc.2017.11.019
Received 6 July 2016; Received in revised form 11 July 2017; Accepted 21 November 2017
0968-090X/ Published by Elsevier Ltd.

freeway segment whenever queues from a segment's off-ramp spilled over and occupied its mandatory exit lane.

To mitigate the freeway congestion caused by excessive off-ramp queue, a category of studies aims to reduce the lane-change maneuvers near the off-ramps. For example, Daganzo et al. (2002) presented a dynamic lane assignment strategy to reduce the frequency of lane-changing maneuvers at the congested off-ramp areas. Based on the field observations, Rudjanakanoknad (2012) proposed two traffic control strategies to increase the off-ramp capacity in the congested area: off-ramp control and prohibiting lane change maneuvers near the off-ramp. To account for drivers' queue-jump behavior at the entry of an off-ramp, Di et al. (2013) proposed a cellular automata-based simulation model to evaluate different configurations of pavement markings around off-ramps. With the same purpose, another category of studies aims to detour the flows to other non-congested areas. For example, Günther et al. (2012) proposed a model to detour some vehicles on the surface streets, and offer the control priority to the off-ramp flows. Hence, their model intends to benefit the off-ramp flows at the expense of surface street users. Spiliopoulou et al. (2013) developed a real-time route diversion model from the user-optimum perspective. Given a detected off-ramp queue spillback, the control module will be executed to detour some off-ramp flows to an alternative route, aiming to prevent queue spillback at off-ramps. Since drivers may ignore the detour instructions, Spiliopoulou et al. (2013) further proposed another control model that calls for temporary off-ramp closure to force the route diversion.

Aside from the aforementioned strategies, a more efficient way to mitigate such off-ramp queue spillover is to control the traffic signals at its connecting local arterial. In review of the literature, it is noticeable that considerable studies have been done on optimizing the corridor control for freeway off-ramp and local arterials. For examples, Messer (1998) provided a control strategy and simulation study to solve traffic congestion at a closely-spaced signalized arterial which has a short distance between its intersections and the interchange exit. Along the same line, Tian et al. (2002) developed an integrated control algorithm, including ramp metering and local signal timings, to improve the performance of a freeway diamond interchange and its neighboring surface street. Li et al. (2009) presented a mixed-integer model for an integrated control between the off-ramp and arterial traffic flows, intending to minimize the queue spillback from an off-ramp to its the freeway mainline. Similarly, Lim et al. (2011) proposed a signal control model to minimize the total delay for off-ramps and their connected arterials. Pei and Zhou (2013) developed a control model to optimize the green time and cycle length at a surface road, based on the off-ramp traffic conditions. Using a two-stage framework, Yang et al. (2015b) proposed a decomposition control model to optimize the intersection signal timings and to concurrently provide signal progression to the competing traffic flows which comes from off-ramps and upstream intersections. In addition, Tian (2007) modelled an integrated control system for a freeway on-ramp and its upstream diamond interchange. The core logic of this study is to control the ramp feeding traffic from the diamond interchange with time-varying signal timings.

Despite the significant research advances reported in literature, several critical issues on this subject remain unsolved. For instance, due to the fluctuation of freeway traffic and the stochastic arrival rate at the off-ramp, an integrated corridor control with pre-timed strategies may not be sufficiently responsive. Using the real-time information, Yang et al. (2014b) provided a control system to prevent the queue spillback at freeway off-ramps. When the potential spillback is predicted, a signal priority with green time extension will be provided to the off-ramp flows, allowing the traffic to quickly pass the downstream intersections. Based on the simulation experiments, the study has demonstrated its effectiveness in preventing off-ramp queue spillovers. However, such system my potentially bring negative impacts to local traffic, and thus may justify the need to implement a complimentary responsive control, such as adaptive signal control which can benefit local intersections.

Using the real-time detected data, adaptive signal control is to dynamically adjust the signal plans and consequently improve the operational efficiency at local intersections. In review of literature, a lot of well-developed systems have been promoted by the transportation researchers. For instance, the Transportation Research Laboratory (Hunt et al., 1982; Day et al., 1998) developed the SCOOT (Spite Cycle and Offset Optimization Technique) system to minimize a pre-defined Performance Index, with the detected data in the form of Cyclic Flow Profiles (CFP). The Sydney Coordinated Adaptive Control System (SCATS), developed by the Department of Main Roads NSW, is a centralized hierarchical signal control system (Lowrie, 1990). Optimized Policies for Adaptive Control (OPAC) is a distributed real-time traffic signal control system that continuously adapts signal timings to minimize a performance function, based on the total intersection delay and vehicle stops over a pre-specified horizon (Gartner, 1983; Gartner et al., 1995; Gartner et al., 2001, 2002). The Real-time Hierarchical Optimizing Distributed Effective System (RHODES) uses a three-level hierarchy to characterize and manage traffic, which can explicitly predict traffic at these levels based on detector and other sensor information (Mirchandani and Head, 2001; Mirchandani et al., 2000). Other well-developed adaptive control systems include PRODYN (Henry et al., 1983) and UTOPIA (Mauro and Di Taranto, 1989).

Following the same line, this study intends to develop a control system which integrates the off-ramp priority control and adaptive signal control at local intersections. To tackle traffic congestions at local intersections so as to prevent the off-ramp queue spillover, the proposed system has been designed with three core control functions: off-ramp queue length estimation, arterial adaptive control, and off-ramp priority control. Specifically, the off-ramp queue length estimation function is used to predict whether a potential queue spillover will occur in the following signal cycle. Based on the detected flow data, the arterial adaptive control system will dynamically adjust intersection signal timings and offsets to reduce the intersection delay as well as provide signal progression to those heavy path-flows. When potential queue spillover is predicted, the off-ramp priority control function will be activated to offer green extension and progression priority to the off-ramp flows.

The remaining part of this paper is organized as follows: the next section will introduce the research background with some field observations and the system framework; Section 3 will introduce the off-ramp queue estimation model; Sections 4 and 5 will illustrate the formulations of adaptive control and off-ramp priority control functions; Section 6 will present the numerical example results and some conclusions along with future research directions will be provided in the last section.

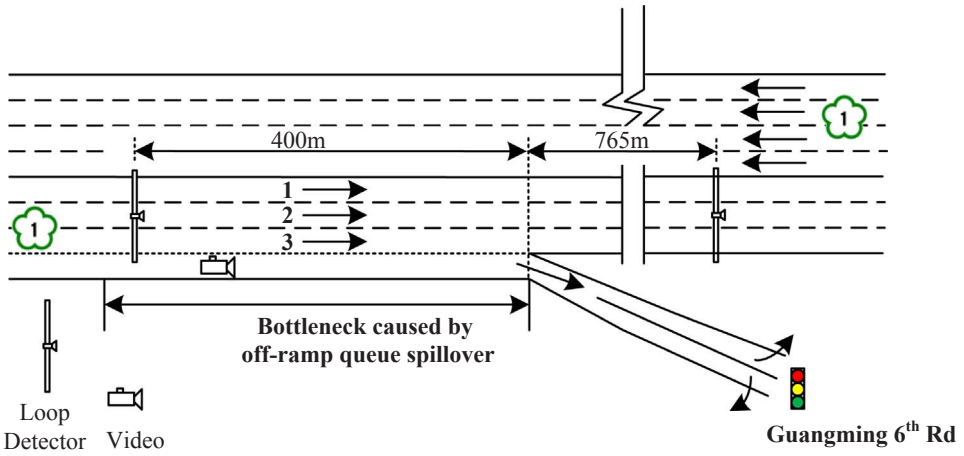

Fig. 1a. The illustration of the detection system at the study site.

2. Research background and system framework

2.1. Research background

To illustrate the interrelations between the off-ramp queue and local traffic, this study selects the freeway segment in Chupei, Taiwan as the study site (Fig. 1a). Two loop detectors are installed at the upstream and downstream of the off-ramp interchanged area and one video detector is deployed to monitor the queue length evolution at the off-ramp. Fig. 1b shows the time-dependent speed profile on each lane at the upstream of the off-ramp. During the period of 18:00 – 20:30, one can observe significant speed drops on all three freeway lanes. Lane 3, nearest to the spillback lane, has dropped its speed to 20 km/h. However, after the traffic passed the off-ramp entry, the speeds on all three lanes can quickly recover to 90 km/h, as shown in Fig. 1c. Also, the presence of queue spillback has also been recorded with the video camera during the congested period.

Based on the data analysis, one can observe a significant speed reduction at the freeway mainline caused by the off-ramp queue spillover. The congestion near the off-ramp would further cause capacity drop, especially when the exit queue spreads over to the freeway mainline. To overcome this issue, the system can either detour vehicles to other nearby off-ramps to reduce the off-ramp flows, or to adjust the downstream signal timings to increase the discharging flows. The former, however, may not be applicable if nearby off-ramps are too far away. Hence, this study focuses on the latter strategy by dynamically adjusting downstream signals with a real-time control strategy.

2.2. System framework

To improve the overall network performance of the entire network, this study developed an integrated control system that can benefit both freeway segment and local intersections. As shown in Fig. 2, before the start of each signal cycle, the off-ramp queue estimation model will be firstly implemented to identify whether potential queue spillover will be occurred. If no, the adaptive signal control function will be activated to adjust the signal timing at each intersection to minimize the total travel delay. Also, a dynamic signal progression model will be adopted to facilitate those heavy path-flows to reach their destinations. When the potential off-ramp queue spillover is predicted, the system will further evaluate the congestion level on freeway mainline and consequently identify if an

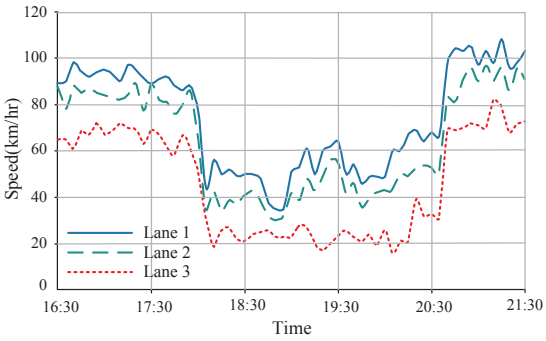

Fig. 1b. Speed obtained by upstream detectors, 16:30–21:30 on April 25, 2013.

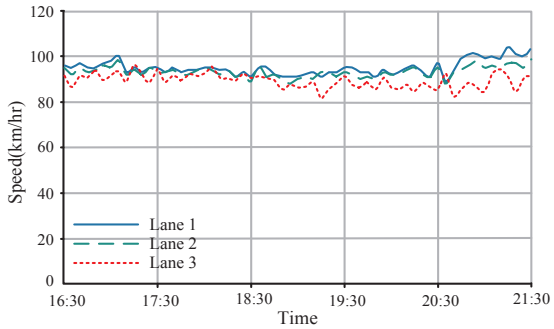

Fig. 1c. Speed obtained by downstream detectors, 16:30–21:30 on April 25, 2013.

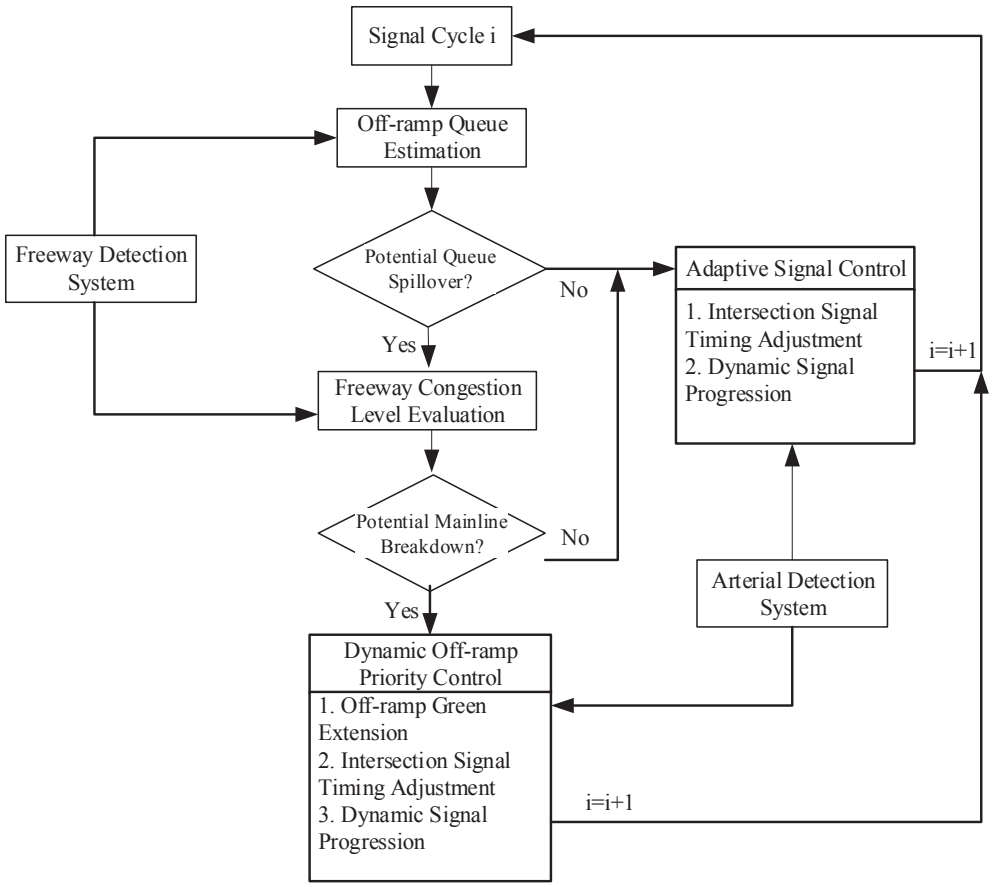

Fig. 2. The framework of the integrated control system.

operational bottleneck will be formed by the off-ramp queue. If yes, the off-ramp priority control function will be activated to discharge the queuing flows on the off-ramp, based on the logic of offering green time extension and progression priority.

3. Off-ramp queue estimation

To develop a reliable off-ramp queue estimation model, Yang et al. (2014a,b) adopted dual-zone detectors for data detection and collections, where each detector can provide two detection zones. Particularly, the short detection zones are used to count traffic flow rates and the information from long detection zone can indicate the presence of traffic queues.

As shown in Fig. 3, dual-zone detectors are implemented at both upstream and downstream of off-ramp. If the upstream detector data detects the queue, a queue spillback warning will be provided to the control system. In contrast, when the off-ramp queue doesn't spillback to the upstream detection zone, the following two models will be implemented under different scenarios:

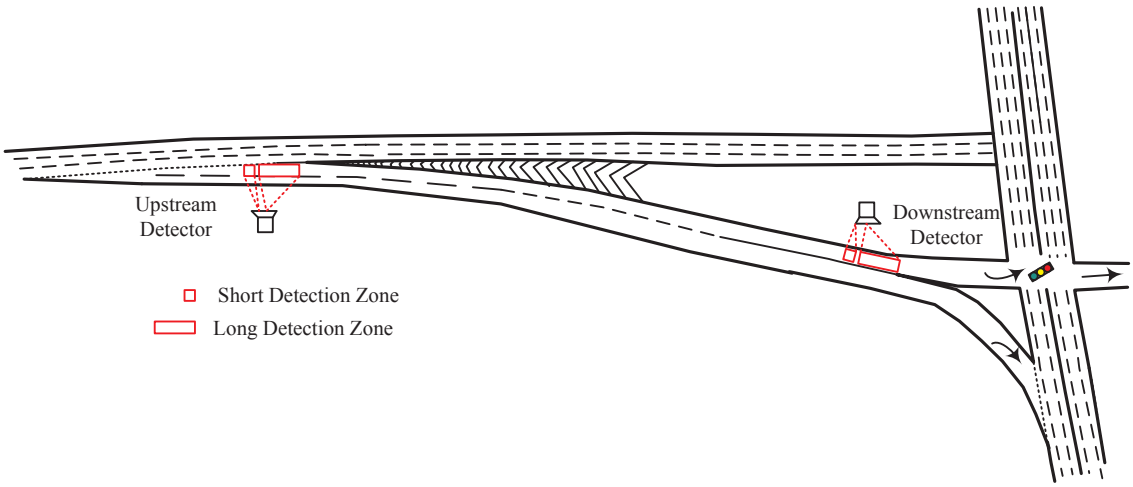

Fig. 3. Location of dual-zone detectors on the target off-ramp.

- Model I: If the data from downstream detector indicates the clearance of off-ramp queue during the green time;
- Model II: If the downstream detector cannot detect the clearance of off-ramp queue during the green time.

3.1. Model 1

Assuming the signal cycle starts with the green phase for off-ramp flows and queue is fully discharged at time interval $\varepsilon(k)$ in signal cycle k, the number of moving vehicles between two detectors equals the number of vehicles which passed the upstream detector during time period $[\varepsilon(k) - t_{off}, \varepsilon(k)]$:

$$\delta(\varepsilon,k) = \sum_{t=\varepsilon-t_{off}}^{\varepsilon} q_{up}(t,k) \tag{1}$$

where $\delta(t,k)$ denotes the number of vehicles on the off-ramp during time interval t in signal cycle k; $q_{up}(t,k)$ denotes the number of vehicles detected by the upstream detector during time interval t in signal cycle k; t_{off} denotes the average travel time from off-ramp upstream detector to the downstream detector, in seconds.

Then, at end of green time, the total number of vehicles between two detectors is calculated by adding the difference between the numbers of the vehicles detected at the upstream and downstream detectors, as expressed below:

$$\delta(g_{off},k) = \delta(\varepsilon,k) + \sum_{t=\varepsilon}^{g_{off}} q_{up}(t,k) - \sum_{t=\varepsilon}^{g_{off}} q_{down}(t,k) \tag{2}$$

where $q_{up}(t,k)$ and $q_{down}(t,k)$ represent the number of vehicles detected during time interval t in signal cycle k by the upstream detector and the downstream detector, respectively; g_{off} denotes the end of green

After that, during the red phase, no queuing vehicle is discharged. Hence, at the end of the cycle, the total number of vehicles between two detectors is estimated by adding number of vehicles passing the upstream detector:

$$\delta(c,k) = \delta(g_{off},k) + \sum_{t=g_{off}}^{c(k)} q_{up}(t,k) \tag{3}$$

where $c(k)$ denotes the common cycle length in signal cycle k, in seconds.

Therefore, the queue length at the end of cycle could be approximately computed by:

$$\tau_{off}(c,k) = \delta(c,k) + \delta_0 \tag{4}$$

where $\tau_{off}(t,k)$ represents the off-ramp queue length during time interval t in signal cycle k, in number of vehicles; δ_0 is a constant, which indicates the number of vehicles stored between downstream detector and signal stop-line.

3.2. Model 2

If residual queue still exists at the end of green time, two cases may be encountered:

(1) The residual queue doesn't reach the downstream detector;
(2) The residual queue has reached the downstream detector.

For the first case, the downstream detector data will be examined first. Assuming that traffic queue has reached the downstream detector at time interval η, which is the time when the long detection zone first detects steady vehicles after the end of green phase, the total number of vehicles between two detectors at the end of cycle is given by:

$$\delta(c,k) = \sum_{t=\eta-t_{off}}^{c(k)} q_{up}(t,k) \tag{5}$$

Similarly, the queue length at the end of cycle could be computed by Eq. (4).

If the residual queue has exceeded the location of downstream detector, the queue length at the end of cycle should be calculated based on the estimated queue length in the last cycle, as well as the flow conservation relation, which is shown below:

$$\tau_{off}(c,k) = \tau_{off}(c,k-1) + \sum_{t=1}^{c(k)} q_{up}(t,k) - \sum_{t=1}^{c(k)} q_{down}(t,k) \tag{6}$$

where $\tau_{off}(c,k-1)$ represents the estimated queue length at the end of last cycle, which should be set to 0 if the queue is detected to be cleared by the long detection zone of the downstream detector.

With Eqs. (1)–(6), the off-ramp queue length at the end of the red time of each cycle can be estimated. Then, at the start of each signal cycle, the system will compare that estimated queue with a pre-determined threshold. The threshold is determined such that, if the estimated queue length reaches it, vehicles would spill back to the freeway mainline during the queue discharging period, given the off-ramp volume. With such a method, data from the dual zone detectors can be used to identify whether potential queue spillover might occur.

4. Adaptive signal control

4.1. Flow detection and estimation

As aforementioned, the adaptive signal control function will be activated when potential off-ramp queue spillover or freeway mainline breakdown is not detected. Hence, such system will take advantage of the real-time information from intersections and adjust signal plans to benefit the local traffic. To provide essential input for the adaptive signal control model, the system would install detectors after the stop bars at each intersection, as shown in Fig. 4. Then the detectors will record the intersection turning flows and send the information to the control system after the completion of each signal cycle.

To provide a proactive signal control, the system will further adopt its flow estimation module. Based on the detected flow rate at each intersection, one may employ a vast body of algorithms in the statistical literature to perform the estimation. An example of methods which is convenient but reasonably effective is the following smoothing approach:

$$q_{i,j}(k) = \frac{1}{m}\sum_{t=1}^{m} q_{i,j}(k-t) \tag{7}$$

where m is the number of previous signal cycles considered; $q_{i,j}(k)$ denotes the number of detected vehicles on link j at intersection i in signal cycle k. The turning flows estimated for each intersection can then serve as the primary input for the adaptive signal control module to compute the cycle length and signal timings. The offsets for all intersections shall also be adjusted accordingly for design of signal progression.

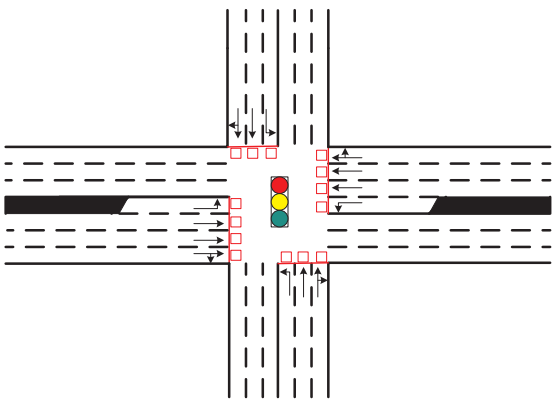

Fig. 4. Illustration of the detection system at each intersection.

4.2. Adaptive signal control

Given the signal phasing design and phase sequence at each intersection, this function will increase or decrease the common cycle length by a pre-determined time interval (e.g., 5 s) after the completion of each control horizon (e.g., 5 min). Similar to the existing adaptive control system such as SCOOT, the function will select the most congested intersection in the arterial for evaluation. Then, the cycle length will be adjusted to maintain the intersection v/c ratio to be within the target threshold (e.g., 80%).

Within each control horizon, an optimization model is further implemented to dynamically adjust signal timings at each intersection. The formulations of such model for intersection i during signal cycle k are summarized as follows:

$$M1: \ Min \ d_i(k) \tag{8}$$

s.t.

$$d_i(k) = \sum_{j=1}^{N} \sum_{t=1}^{c} \tau_{i,j}(t,k)\Delta t \tag{9}$$

$$\mu_{i,j}(t,k) = \frac{1}{c} q_{i,j}(k) \quad \forall j,t \tag{10}$$

$$r_{i,j}(t,k) = \begin{cases} s_{i,j}\Delta t & if \ green \\ 0 & if \ red \end{cases} \quad \forall j,t \tag{11}$$

$$\tau_{i,j}(0,k) = \tau_{i,j}(c,k-1) \quad \forall j \tag{12}$$

$$\tau_{i,j}(t,k) = Max\left[\tau_{i,j}(t-1,k) + \mu_{i,j}(t,k) - r_{i,j}(t,k),\ 0\right] \quad \forall j,t \tag{13}$$

$$\sum_{p=1}^{Np_i} (g_{i,p}(k) + l_{i,p}(k)) = c(k) \tag{14}$$

$$g_{i,p,\min} \leqslant g_{i,p}(k) \leqslant g_{i,p,\max} \tag{15}$$

$$g_{i,p}(k-1) - \Delta g_i \leqslant g_{i,p}(k) \leqslant g_{i,p}(k-1) + \Delta g_i \tag{16}$$

In the above optimization model, the control objective (Eq. (8)) is to minimize the total intersection delay, where $d_i(k)$ denotes total intersection delay at intersection i in signal cycle k, in seconds; N denotes the number of intersections on the target arterial. Eq. (9) denotes the total delay with the queue length, $\tau_{i,j}(t,k)$, on all intersection links and the length of time interval Δt. Eq. (10) is used to estimate the vehicle arrival rate on link j at intersection i during time interval t in signal cycle k in vehicles per second, $\mu_{i,j}(t,k)$, on the links during each time interval, based on the number of detected vehicles, $q_{i,j}(k)$. Eq. (11) estimates the total number of departing vehicles from each link, where $s_{i,j}$ indicates the saturation flow rate and $r_{i,j}(t,k)$ denotes departure rate on link j at intersection i during time interval t in signal cycle k, in vehicles per second. Eq. (12) approximates the initial link queue at the start of a signal cycle, where $\tau_{i,j}(t,k)$ represents queue length on link j at intersection i during time interval t in signal cycle k, in number of vehicles. The queue length at time interval t depends on the queue length during last time interval, the arrival flow, and departure flow as denoted by the first term in the bracket of Eq. (13). Eq. (14) ensures that the summation of effective green times and lost times equals the cycle length, where $g_{i,p}(k)$ denotes the assigned green time for phase p at intersection i in signal cycle k in seconds; $l_{i,p}(k)$ denotes the lost time for phase p at intersection i in signal cycle k in seconds and Np_i denotes the set for all signal phases at intersection i. Eq. (15) sets the minimal and maximal green times for each phase, denoted by $g_{i,p,\min}$ and $g_{i,p,\max}$. To stabilize the green time transitions between phases, one shall let the adjustment of signal timings be constrained within a pre-calibrated interval (e.g., 6 s), as shown in Eq. (16), where Δg_i denotes the maximal allowed green time difference between two signal consecutive cycles at intersection i, in seconds.

The algorithm for the proposed M1 model to be efficiently solved for on-line applications is presented below:

Step 1: Initialization. Let $p = 1$ and get the green time of each phase at the previous signal cycle;

Step 2: For phase p, change the green time by α seconds (could be negative or positive) by solving the following sub-problem:

$$\begin{aligned} &\alpha = \arg\min\{d_i(k);\ m \in N_p,\ m \neq p\} \\ &s.t. \quad g_{i,p}(k) = g_{i,p}(k-1) + \alpha \\ &\quad g_{i,m}(k) = g_{i,m}(k-1) - \alpha \\ &\quad -\Delta g_i \leqslant \alpha \leqslant \Delta g_i \\ &\quad g_{i,p,\min} \leqslant g_{i,p}(k) \leqslant g_{i,p,\max} \\ &\quad g_{i,m,\min} \leqslant g_{i,m}(k) \leqslant g_{i,m,\max} \end{aligned} \tag{17}$$

Step 3: Let $p = p + 1$. If $p > |Np_i|$, stop; otherwise go back to Step 2.

It is noticeable that the sub-problem (17) in Step 2 is to transfer a few seconds of green time between the target phase p and one of other phases. To solve this sub-problem and ensure the computation efficiency for on-line applications, the system can use a gradient searching approach, similar to the heuristic in SCOOT, to find the optimal value for α. And the solution process could be explained as follows:

// initialization:

$opt d_i(k) = \{\sum_{j=1}^{N_j}\sum_{t=1}^{c}\tau_{i,j}(t,k)\Delta t \mid g_{i,p}(k) = g_{i,p}(k-1) \ \forall p\}$; $d_i(k) = 0$;

// signal timing adjustment for phase p

// Step 1: find the adjustment direction

$\alpha = 1$;

$d_i(k) = \min_{m \neq p}\left\{\sum_{j=1}^{N_j}\sum_{t=1}^{c}\tau_{i,j}(t,k)\Delta t \mid g_{i,p}(k) = g_{i,p}(k-1) + \alpha, g_{i,m}(k) = g_{i,m}(k-1) - \alpha\right\}$

if $d_i(k) < opt d_i(k)$

{$opt d_i(k) = d_i(k)$;

$direction = 1$;

}

else

{$\alpha = -1$;

$d_i(k) = \min_{m \neq p}\left\{\sum_{j=1}^{N_j}\sum_{t=1}^{c}\tau_{i,j}(t,k)\Delta t \mid g_{i,p}(k) = g_{i,p}(k-1) + \alpha, g_{i,m}(k) = g_{i,m}(k-1) - \alpha\right\}$;

if $d_i(k) < opt d_i(k)$

{$opt d_i(k) = d_i(k)$;

$direction = -1$;

}

else

{$direction = 0$; break}

}

// continue to adjust the green time along the direction until no delay reduction is found

$\alpha = direction$;

$d_i(k) = \min_{m \neq p}\left\{\sum_{j=1}^{N_j}\sum_{t=1}^{c}\tau_{i,j}(t,k)\Delta t \mid g_{i,p}(k) = g_{i,p}(k-1) + \alpha, g_{i,m}(k) = g_{i,m}(k-1) - \alpha\right\}$;

do while ($d_i(k) <= opt d_i(k)$)

{$\alpha = \alpha + direction$;

$opt d_i(k) = d_i(k)$;

$d_i(k) = \min_{m \neq p}\left\{\sum_{j=1}^{N_j}\sum_{t=1}^{c}\tau_{i,j}(t,k)\Delta t \mid g_{i,p}(k) = g_{i,p}(k-1) + \alpha, g_{i,m}(k) = g_{i,m}(k-1) - \alpha\right\}$

}

The algorithm first calculates the intersection delay based on the signal timing at the last time interval (i.e., 5 min). Increasing (or reducing) one second for phase p will determine whether the intersection delay can be reduced. If yes, the direction that causes delay reduction will be recorded and further adjustment along this direction will be conducted until the delay cannot be further reduced. By implementing such an algorithm, the entire solution process for the optimization model (see Eqs. (8)–(16)) can be completed efficiently, which satisfies the need of on-line applications.

4.3. Dynamic signal progression control

Aside from dynamically adjusting signal timings at each intersection, another essential issue associated with the adaptive signal control is to provide signal progression to heavy traffic. In review of the literature, providing two-way signal progression (e.g., MAXBAND by Little et al., 1981) has long been viewed as one of the most effective control strategies. However, at the off-ramp interchanged area, the traffic volumes, that need to take these paths comprising both turning and through movements, are likely to be at the same level or even higher than the through volume along the arterial. Fig. 5 presents an example of such traffic systems in Chupei, Taiwan, where the heavy turning volumes from-or-to the on-ramp and off-ramps are in conflict with through traffic. A further field survey and analysis has revealed that the traffic patterns along the arterial segment are the collective manifestation of five congested path-flows.

Thus, depending on the required turning volume at each arterial intersection, the conventional progression design for through traffic flows may not be adequate to contend with the potential queue spillback and resulting stop-and-going conditions, especially for arterials having a short link and bay length between intersections. To deal with this issue, Yang et al. (2015a) developed a multi-path progression model to concurrently offer certain green band to those critical path-flows. Based on the extensive numerical

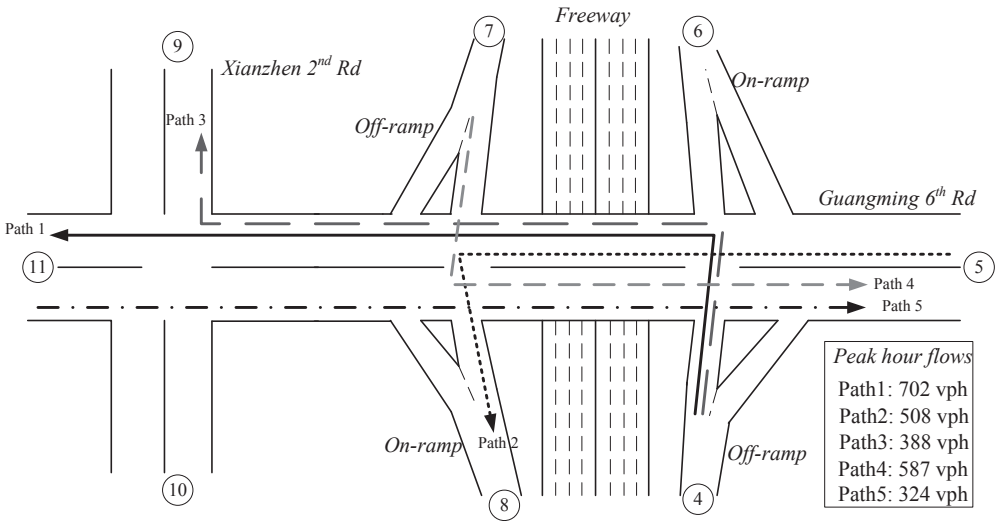

Fig. 5. Critical traffic paths at the off-ramp interchanged network in Chupei, Taiwan.

investigation with field data, that study has confirmed the need of providing signal progression to multiple heavy path-flows.

Following the same concept of multi-path progression, the proposed system in this study will extend it to a dynamic progression control function in responds to the changing of signal timings at each intersection. For the convenience of discussion, this study denotes $t_{i,l,1}$ and $t_{i,l,2}$ as the start and end of green for path-flow l at intersection i. Other key notations are shown in Fig. 6.

Given the cycle length and signal timings generated from the adaptive signal control function, the dynamic signal progression model could be summarized as follows:

$$M2:\ Max \sum_i \sum_l f_l(k) b_{i,l}(k) + \sum_i \sum_l \overline{f}_l(k) \overline{b}_{i,l}(k) \tag{18}$$

s.t.

$$b_{i,l}(k) = Max[Min(t_{i+1,j,2}(k), t_{i,j,2}(k) + t_{i,i+1}(k)) - Max(t_{i,j,1}(k) + t_{i,i+1}(k), t_{i,j,1}(k)), 0] \tag{19}$$

$$\overline{b}_{i,j}(k) = Max[Min(t_{i,j,2}(k), t_{i+1,j,2}(k) + t_{i+1,i}(k)) - Max(t_{i,j,1}(k), t_{i,j,1}(k) + t_{i+1,i}(k)), 0] \tag{20}$$

$$t_{i,l,1}(k) = \sum_q \sum_p \zeta_{i,l,p} \varphi_{p,q} g_{i,p}(k) + \theta_i(k) \tag{21}$$

$$t_{i,l,2}(k) = \sum_q \sum_p \zeta_{i,l,p} \varphi_{p,q} g_{i,p}(k) + \sum_p \zeta_{i,j,p} \varphi_{p,q} g_{i,p}(k) + \theta_i(k) \tag{22}$$

$$\theta_i(k-1) - \Delta\theta_i \leqslant \theta_i(k) \leqslant \theta_i(k-1) + \Delta\theta_i \tag{23}$$

The control objective (Eq. (18)) is to maximize the sum of weighted green band between all adjacent intersections for all path-flows, where $b_{i,l}(k)$ ($\overline{b}_{i,l}(k)$) denotes green bandwidth for the outbound (inbound) path-flow l at between intersections i and $i-1$, in seconds and $f_l(k)$ ($\overline{f}_l(k)$) indicates the corresponding weighting factor. Also note that those weighting factors could be determined by

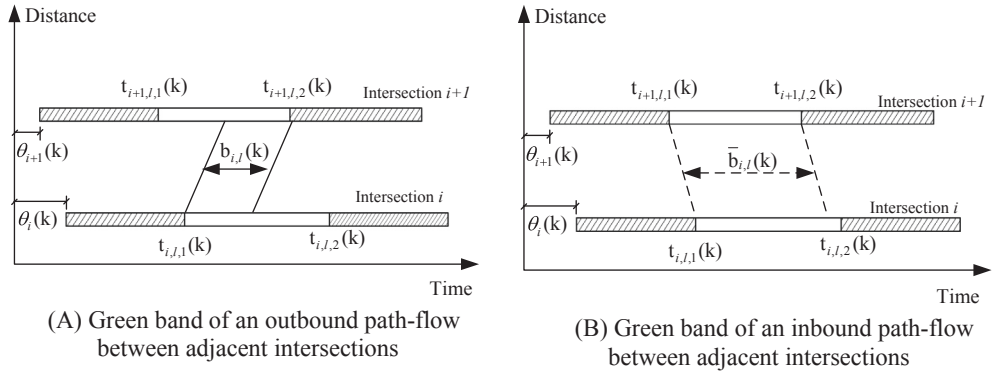

Fig. 6. Key notations for the green band of path-flows.

the traffic volumes along different paths. Eqs. (19) and (20) are used to compute the corresponding green bandwidth for an outbound and an inbound path-flow, respectively, between two adjacent intersections i and $i + 1$. The left and right edges can be determined by the start and end of the green phases at two intersections. Eqs. (21) and (22) are implemented to compute the start and end of green for a path l at intersection i, based on the intersection offset, signal timings, and phasing design, where $\theta_i(k)$ denotes the signal offset at intersection i in signal cycle k in seconds; $\xi_{i,l,p}$ is a binary parameter which equals "1" if path l receives green in phase p at intersection i, equals "0" otherwise; and $\varphi_{p,q}$ is a binary phase sequence parameter which equals "1" if phase p is before q, equals "0" otherwise. Eq. (23) will constrain the change of offset within a certain range (e.g., 6 s), where $\Delta\theta_i$ denotes the maximal allowed offset difference between two signal consecutive cycles at intersection i in seconds.

To solve the proposed optimization model shown by Eqs. (18)–(23), a dynamic programming solution algorithm is adopted in this study. Given Eq. (23), the feasible solution set for the new offset at each intersection is given as follows:

$$\Theta_i(k) = \{\theta_i(k-1)-\Delta\theta_i,\ \theta_i(k-1)-\Delta\theta_i + 1,\ \cdots,\ \theta_i(k-1) + \Delta\theta_i\} \tag{24}$$

Also the total green bandwidths of all path-flows between intersections $i-1$ and i, $B_i(\theta_i)$, could be calculated by:

$$B_i(\theta_i) = \sum_l \beta_{i-1,l,p}\beta_{i,l,p}\phi_l(k)b_{i,l}(k) + \sum_l \beta_{i-1,l,p}\beta_{i,l,p}\overline{\phi}_l(k)\overline{b}_{i,l}(k) \tag{25}$$

where $\beta_{i,j,p}$ is a binary parameter which equals "1" if link j receives green in phase p at intersection i, equals "0" otherwise; the bandwidth, $b_{i,l}(k)(\overline{b}_{i,l}(k))$, for each outbound (inbound) path-flow could be obtained by Eqs. (19)–(22).

Denotes $f_i(\cdot)$ as the accumulated performance measure, then the solution algorithm is summarized as follows:

Step 1: set $i = 1$, $\theta_1(k) = 0$, and $f_i(0) = 0$;
Step 2: $i = i + 1$;
$f_i(\theta_i^*(k)) = \min_{\theta_i(k)}\{f_{i-1}(\theta_{i-1}^*(k)) + B_i(\theta_i(k))|\theta_i \in \Theta_i(k)\}$
Record $\theta_i^*(k)$ as the optimal solution in Step 2.
Step 3: if $i < N_i$, go to Step 2.
Else, Stop.

---

5. Dynamic off-ramp priority control

As shown in Fig. 2, when potential off-ramp queue spillover is detected by the queue estimation function, the system needs to further evaluate the congestion level of freeway. Based on the detected flow data obtained from the freeway upstream site, the system will compare such information with a pre-defined threshold and identify whether potential mainline breakdown might be occurred.

When such mainline breakdown is predicted, the dynamic off-ramp priority control function will be activated. To prevent the occurrence of off-ramp queue spillover, the function has two control strategies: (1) increasing of green time for the off-ramp flows at the downstream intersection; (2) providing signal progression priority to those path-flows which come from the target off-ramp. Similar to the adaptive signal control function introduced above, the off-ramp priority control function also includes two core steps, signal timing adjustment and signal progression design.

5.1. Adaptive signal control with off-ramp priority

To limit the negative impact to local traffic, the real-time adaptive control system needs to reduce the activation frequency for such priority control. Furthermore, the corresponding extension for the minimal green in signal cycle k shall ensure the prevention of queue spillover until the end of the following signal cycle. Eqs. (26) and (27) show those two constraints for the maximal queue length during cycle k and $k + 1$, respectively::

$$\tau_{off}(c,k-1)-s_{off}(g_{off}(k) + e_{off}(k)) + q_{off}(k) = \tau_{off}(c,k) < L_{off} \tag{26}$$

$$\tau_{off}(c,k)-s_{off}g_{off}(k+1) + q_{off}(k+1) = \tau_{off}(c,k+1) < L_{off} \tag{27}$$

where L_{off} shows the maximum number of vehicles stored on the off-ramp, s_{off} represents saturation flow rate for off-ramp flows, in vehicles per second, $g_{off}(k)$ denotes the total green time assigned to the target off-ramp flows in signal cycle k in seconds; $e_{off}(k)$ denotes green extension time assigned to the target off-ramp flows in signal cycle k in seconds. Eqs. (26) and (27) would make sure that the queue length at the end of either cycle would not be longer than the off-ramp.

Hence, the minimum green extension time for cycle k, $e_{off}^{\min}(k)$, could be determined by:

$$e_{off}^{\min}(k) = \frac{L_{off}-\tau_{off}(c,k-1) + Max\left[s_{off}g_{off}(k)-q_{off}(k), \sum_{m=k}^{k+1}(s_{off}g_{off}(m)-q_{off}(m))\right]}{s_{off}} \tag{28}$$

Then, the adaptive signal control model with off-ramp priority could be summarized as follows:

$M3$: $Min\ d_i(k)$

s.t.

Eqs. (9)–(16)

$$g_{off}(k) - g_{off}(k-1) \geqslant e_{off}^{\min}(k) \tag{29}$$

where Eq. (29) is an additional constraint that guarantee the minimum green extension time is satisfied.

Also by replacing the minimum green time for off-ramp flows with $e_{off}^{\min}(k) + g_{off}(k-1)$, one can use the similar solution algorithm for model M1 to solve model M3.

5.2. Dynamic signal progression control with Off-ramp priority

With the green extension, the real-time adaptive system shall also activate the signal progression module to revise the offsets to provide priority control to the off-ramp path-flows. Specifically, a minimal total green bandwidth for those path-flows, $B_{off}^{\min}$, shall be sufficient to discharge the queuing off-ramp vehicles. Hence, the control model could be summarized as follows:

$$M4:\ Max \sum_i \sum_l \phi_l(k) b_{i,l}(k) + \sum_i \sum_l \overline{\phi}_l(k) \overline{b}_{i,l}(k)$$

s.t.

Eqs. (19)–(22)

$$\sum_{l \in \Gamma_{off}} b_{i,l}(k) > B_{off}^{\min} \tag{30}$$

$$\sum_{l \in \Gamma_{off}} \overline{b}_{i,l}(k) > B_{off}^{\min} \tag{31}$$

Similar to the control model M2, the solution algorithm with dynamic programming for M4 is given below:

Step 1: set $i = 1$, $\theta_1(k) = 0$, and $f_i(0) = 0$;

Step 2: $i = i + 1$;

$$f_i(\theta_i^*(k)) = \min_{\theta_i(k)} \left\{ f_{i-1}(\theta_{i-1}^*(k)) + B_i(\theta_i(k)) \,\middle|\, \theta_i \in \Theta_i(k); \sum_{l \in \Gamma_{off}} b_{i,l}(k) > B_{off}^{\min}; \sum_{l \in \Gamma_{off}} \overline{b}_{i,l}(k) > B_{off}^{\min} \right\}$$

Record $\theta_i^*(k)$ as the optimal solution in Step 2.

Step 3: if $i < N_i$, go to Step 2.

Else, Stop.

Notably, although the off-ramp priority control based on estimated queue length is reactive, the activation threshold in terms of number of queuing vehicles shall be smaller than the storage capacity of off-ramp. As such, the system can take actions to change signal settings before an actual queue spillover occurs.

6. Numerical examples

6.1. Experimental designs

To evaluate the potential of the proposed models for real-world applications, this study has further selected an arterial segment of three intersections in Chupei, Taiwan for case study. As shown in Fig. 7(A), during PM peak hours, heavy traffic flows will take the off-ramp to enter the Guanming 6 th Rd, which constitutes several turning paths of heavy volumes on the arterial along with the local through traffic.

To analyze the demand patterns at the study site, the research team at the National Chiao Tung University (NCTU) in a project sponsored by Ministry of Communications and Transportation, has completed a field survey from 16:30 to 21:30 on April 24, 2013. The collected data includes:

(1) Freeway northbound flow rate along with its turning ratios at the off-ramp (Node 4);
(2) Traffic volume in each lane group at each intersection shown in Fig. 8;
(3) Maximum Queue length per cycle at critical arterial links. Using the node number in Fig. 8, these critical links are: 1 → 2, 2 → 3, 5 → 1, 8 → 3, 9 → 3, 10 → 3, 3 → 2 and 2 → 1.
(4) Current signal timings, including cycle length, green splits and offsets.

Based on the collected data, they also performed an OD estimations and supplemental surveys on the target arterial segment, and identified five critical paths (see Fig. 7(B)). Also to evaluate the effectiveness of the proposed system in preventing freeway

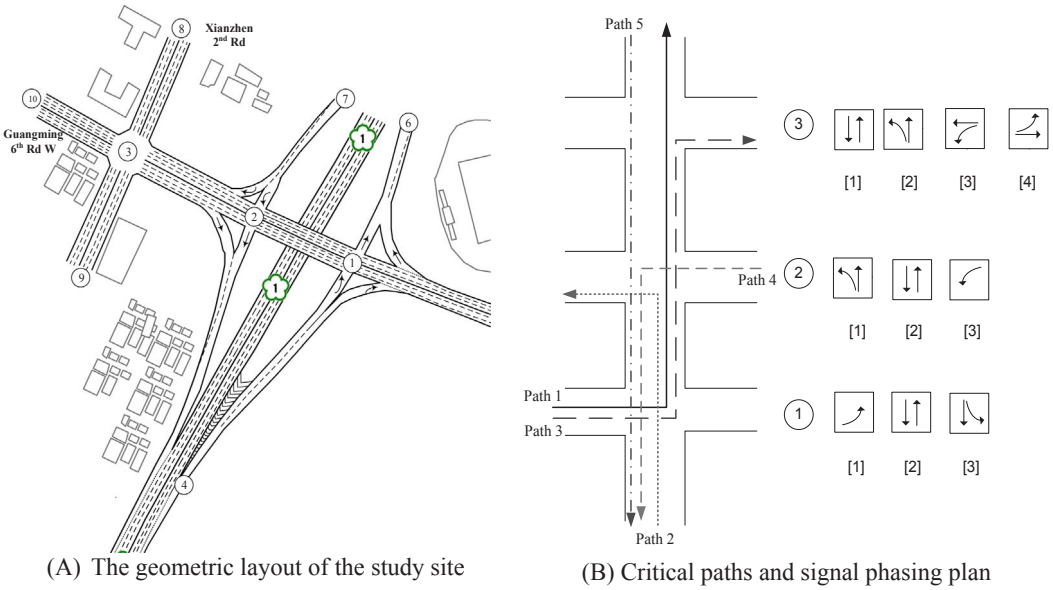

(A) The geometric layout of the study site (B) Critical paths and signal phasing plan

Fig. 7. The general information of the study site. (A) The geometric layout of the study site; (B) Critical paths and signal phasing plan.

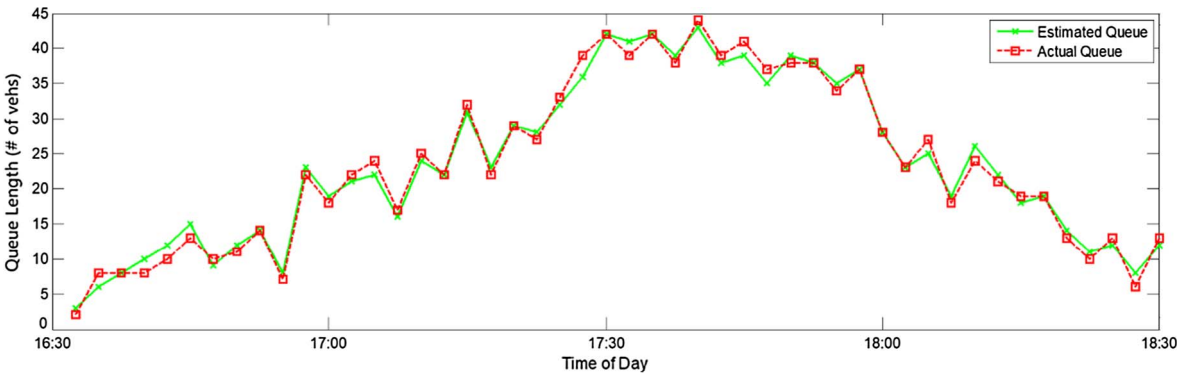

Fig. 8. Comparison of estimated and actual queue length at the target off-ramp.

Table 1
The two-hour demand patterns for the three intersections.

Time	Intersection	Westbound			Northbound			Eastbound			Southbound		
		L	T	R	L	T	R	L	T	R	L	T	R
16:30–17:00	1	/	665	/	995	/	968	443	840	/	/	/	/
	2	269	1391	/	/	/	/	/	921	/	362	/	403
	3	287	872	635	/	238	300	82	653	91	658	286	69
17:00–17:30	1	/	824	/	1090	/	1073	518	976	/	/	/	/
	2	478	1506	/	/	/	/	/	907	/	587	/	672
	3	332	1056	790	/	274	451	82	834	91	729	272	74
17:30–18:00	1	/	924	/	1090	/	1073	518	976	/	/	/	/
	2	508	1506	/	/	/	/	/	907	/	587	/	672
	3	332	1056	790	/	274	451	82	834	91	729	272	74
18:00–18:30	1	/	786	/	1050	/	1011	441	968	/	/	/	/
	2	418	1418	/	/	/	/	/	857	/	551	/	729
	3	363	962	822	/	288	371	88	832	86	761	354	64

Table 2a
Percentage difference between simulation and field volume data.

Intersection no.	Approach			
	WB	NB	EB	SB
1	1%	0.6%	2%	N/A
2	0.9%	N/A	2%	0.2%
3	2%	3%	0.6%	1%

breakdown caused by off-ramp queue spillover, the traffic volumes collected during the two-hour PM peak period are selected for the case study, where the half-hour aggregate turning volumes at each intersection are summarized in Table 1. However, to simulate the traffic fluctuation in practice, this study directly implemented the 5-min flow for system evaluation.

According to the collected data, the values of those control parameters in the proposed system are listed follows:

- The length of time interval Δt is set to be 1 s;
- The average travel time t_{off} between two off-ramp detectors is 15 s;
- The saturation flow rate at all intersections $s_{i,j}$ is 1700 vehicles per hour;
- The green lost time $l_{i,p}$ for each phase is 3 s;
- The minimum and maximum green time, $g_{i,p,\min}$ and $g_{i,p,\max}$, for each phase is 8 s and 100 s, respectively;
- The maximal allowed green time Δg_i difference between two consecutive signal cycles is 6 s;
- The maximal allowed offset difference $\Delta\theta_i$ between two consecutive cycles is 4 s;
- The storage capacity of the off-ramp link L_{off} is 45 vehicles;
- The number of signal cycles, m, for moving average flow prediction is 10;
- The progression weighting factors of five path-flows are 0.3, 0.2, 0.2, 0.2, and 0.1, respectively.
- The weighting factors for off-ramp path-flows (Path 1 and Path 3) are changed to 0.4 when priority control is granted.

To demonstrate the effectiveness of the proposed system, this study concurrently evaluates three systems for comparison:

(1) Pre-timed Control System: using the aggregate data presented in Tables 2a and 2b, the signal optimization model and multi-path progression model by Yang et al. (2015a) are implemented to design the signal plans. The green times and offset at each intersection remains unchanged during the control period.
(2) Adaptive Control System: only the proposed adaptive signal control model and dynamic signal progression model are implemented in this system.
(3) Proposed System: following the control logic shown in Fig. 2, off-ramp queue estimation function, adaptive control function, and off-ramp priority control function are integrated in this system.

6.2. Systems evaluation with simulation

To evaluate the network performance before and after the on-line priority controls, a simulation network is developed with VISSIM. Recognizing that a simulation system is useful only if it can faithfully reflect the behavior of its target driving populations, this study has performed the calibration by minimizing the difference between simulated and field-collected queues as well as flow rates. The calibration results for VISSIM simulation are listed is Tables 2a and 2b.

Since the proposed integrated real-time system may activate the off-ramp priority control when off-ramp queue spillover is predicted, its effectiveness may vary with the estimation accuracy of the off-ramp queue model. With the well-calibrated simulation platform, the comparison between the estimated off-ramp and actual queues (at the end of red phase), are shown in Figs. 8 and 9, respectively.

As shown in Fig. 8, one can observe that the off-ramp queue length at the end of each signal cycle show a tendency of increasing with off-ramp flows. During the peak period (17:15–18:00), the queue length can reach up to 44 vehicles, which is quite close to the off-ramp storage capacity (i.e., 48 vehicles). However, with the priority control function, no spillover has been detected in this case. Also by comparing the estimated queue with actual queue, no significant difference could be observed here. To further analyze the

Table 2b
Adjusted VISSIM parameters.

Parameters	Value
Average stand still distance (Urban)	3.22 ft
Maximum deceleration (Lane Change)	-14.99 ft/s^2
Accepted deceleration (Lane Change)	-6.00 ft/s^2
Maximum deceleration for cooperative braking	-14.99 ft/s^2

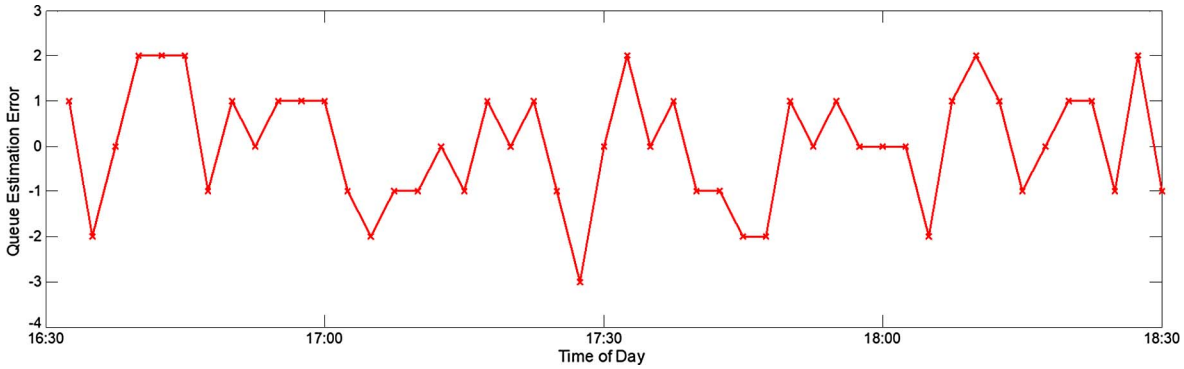

Fig. 9. The estimation errors of the off-ramp queue estimation model.

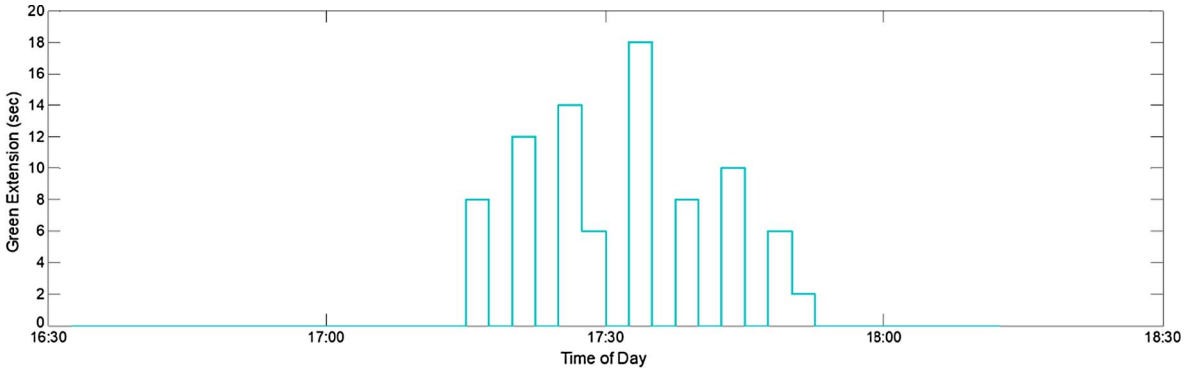

Fig. 10. Green extension time granted to the off-ramp flows.

estimated errors produced by the proposed model, Fig. 9 shows that the differences between the estimated and actual queue lengths fall within the range $[-3, 2]$ vehicles, which is acceptable for operations.

Fig. 10 shows the activation frequency of the off-ramp priority control along with the green extension granted to the off-ramp flows. As revealing in the graphical results, the priority function is frequently activated during 17:25–17:35 (due to the bursty traffic) and the maximal extended green time is only 18 s. However, with such a function, the off-ramp queue spillover can be successfully prevented, as evidenced by the results shown in Fig. 8.

6.3. Experimental results

6.3.1. Evaluation of the freeway mainline performance

Fig. 11 shows the results that both pre-timed control and adaptive control systems fail to prevent the queue spillover at the target off-ramp, and the travel time along the freeway mainline segment has increased significantly over the congested time period (i.e., 17:15–18:00). However, with the off-ramp priority control function, the freeway mainline flows under the proposed integrated

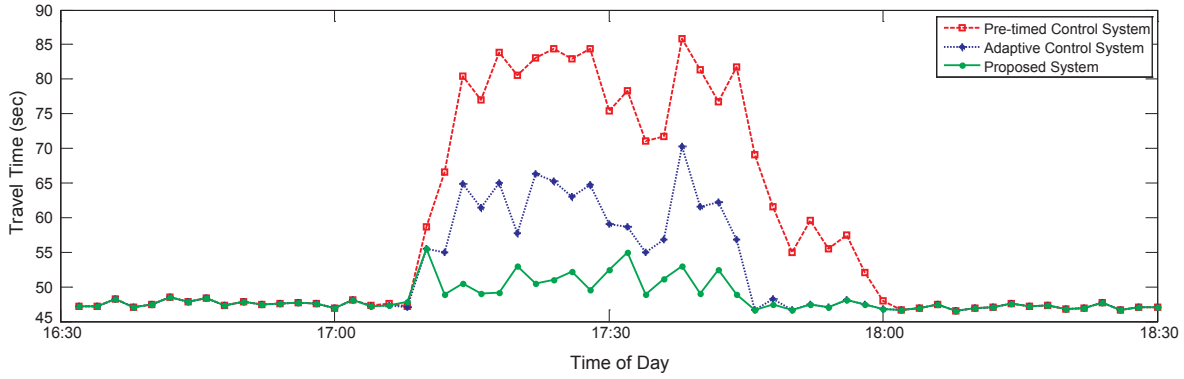

Fig. 11. The time-dependent travel time along the freeway mainline.

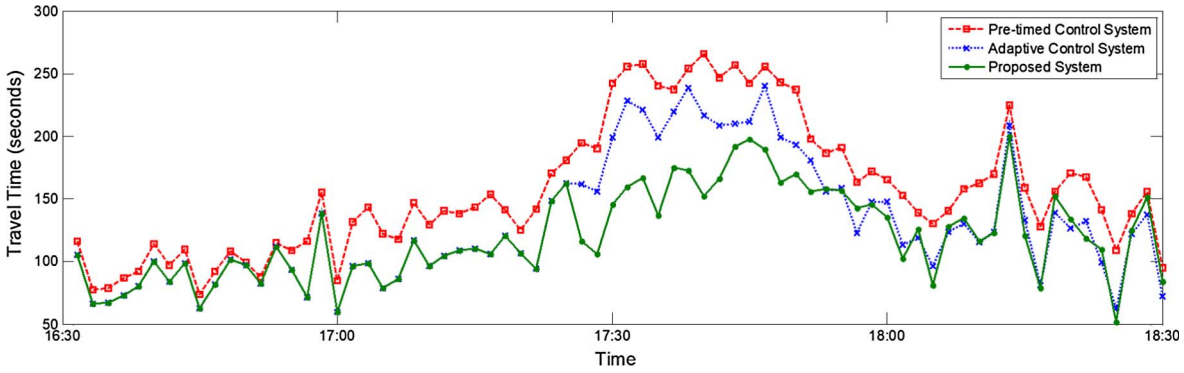

Fig. 12a. The time-dependent travel time along path 1.

system can still maintain a relatively higher travel speed during that period, and an insignificant increase in the freeway travel time. Hence, the experimental results with the simulation have shown that the proposed control strategies are likely to yield satisfactory results, and successfully discharge the off-ramp queue to prevent the excessive traffic spillover.

6.3.2. Evaluation of the critical path-flows

This subsection evaluates the travel times among those critical path-flows from both off-ramp and local arterial. Compared with the pre-timed control system, the other two systems can produce much lower travel time along Path 1, as evidenced by the results in Fig. 12a. This is due to the fact that the dynamic signal progression function can effectively adjust the intersection offset in response to the change in traffic flow patterns. Also, the proposed real-time system can outperform the adaptive control system since it offers Path-1 with green time extension and progression priority when a potential freeway breakdown caused by the off-ramp queue spillover has been predicted. Similar observations could also be found in Fig. 12c since Path-3 shares most signal phases with Path-1.

Fig. 12b shows the comparison of travel times along Path-2. Obviously, the adaptive control system can still outperform the pre-timed system in reducing travel time. However, with the proposed integrated system, the travel time along this path has been increased during the peak-period (i.e., 17:15–18:00). This is due to the fact that with the green extension time granted to the off-ramp flows, the green times for other traffic movements on the arterial will consequently be reduced. Also, the off-ramp flows along both Path-1 and Path-3 could receive progression priority when the control function is activated, which can bring some negative benefits to the traffic along Path-2. Similar observations could also be found in Fig. 12d. Also note that although Path-4 is from the south-bound off-ramp, it is not considered for priority control in this system since no queue spillover has been observed during the control period at the study site.

Fig. 12e further shows that the travel time differences along Path 5 with different models are not significant, even though the proposed model may sacrifice some operation benefits of the local traffic when granting priority control to the off-ramp flows. By analyzing the simulation results, it is noticeable that most traffic volumes along Path 5 have utilized only half of its green band due to its low flow rate. Hence, the provided green bands by the pre-timed control system and adaptive control system have exceeded the need of traffic volume along Path 5, which results in insignificant improvement on travel time, as shown in Fig. 12e.

In conclusion, the adaptive control systems, as expected, can efficiently outperform the pre-timed system in reducing travel times for vehicles along most critical paths. Moreover, the proposed integrated system can successfully prevent the off-ramp queue spillover to the freeway mainline with activation of the priority control function. To further evaluate the systems' operational efficiency over

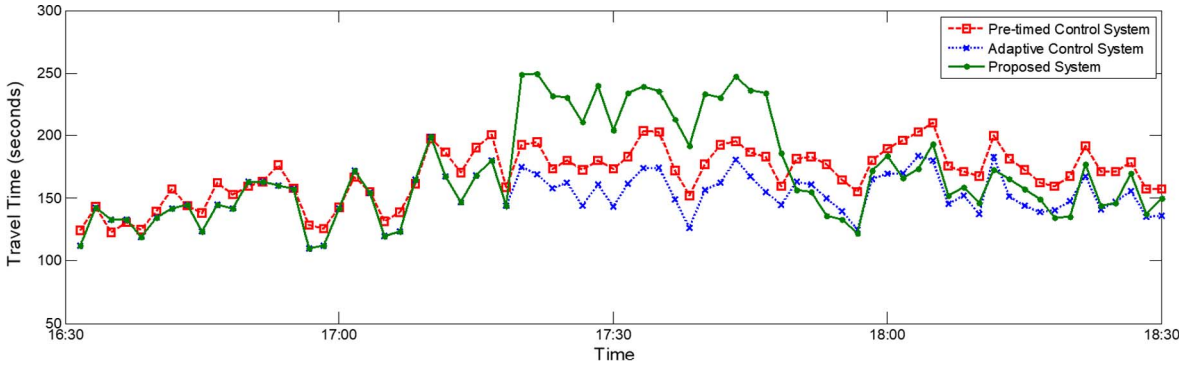

Fig. 12b. The time-dependent travel time along path 2.

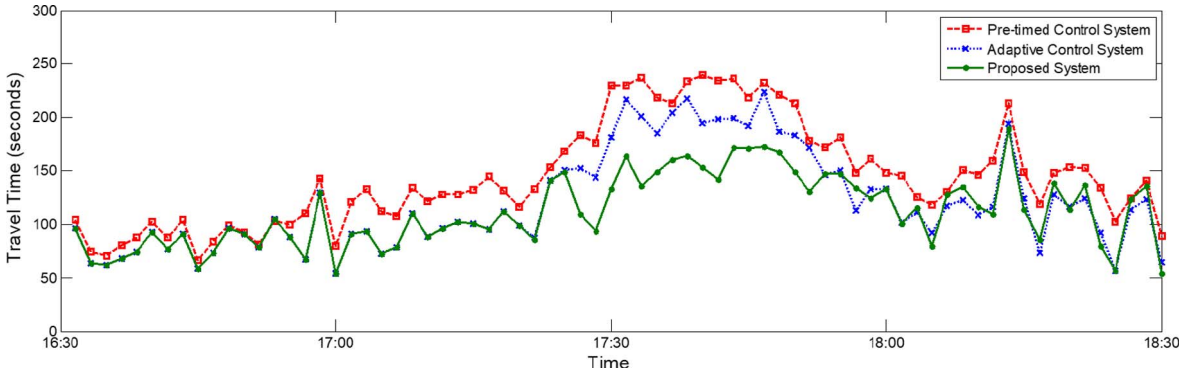

Fig. 12c. The time-dependent travel time along path 3.

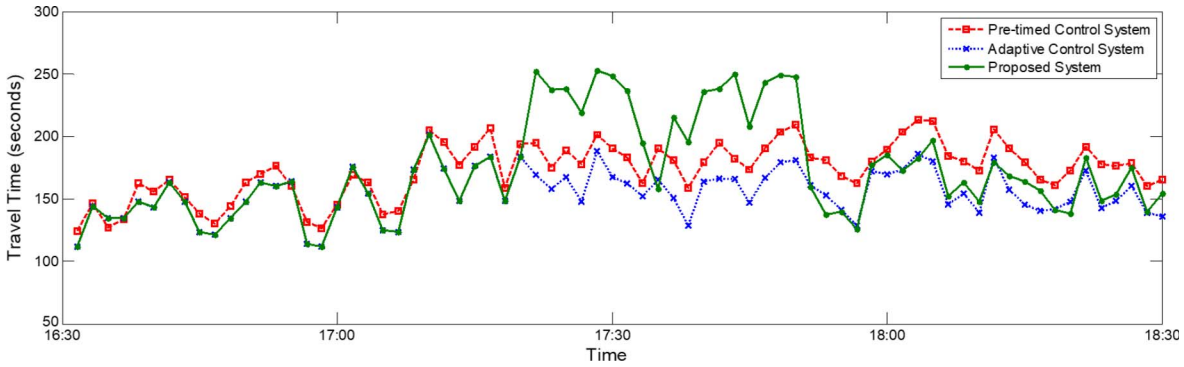

Fig. 12d. The time-dependent travel time along path 4.

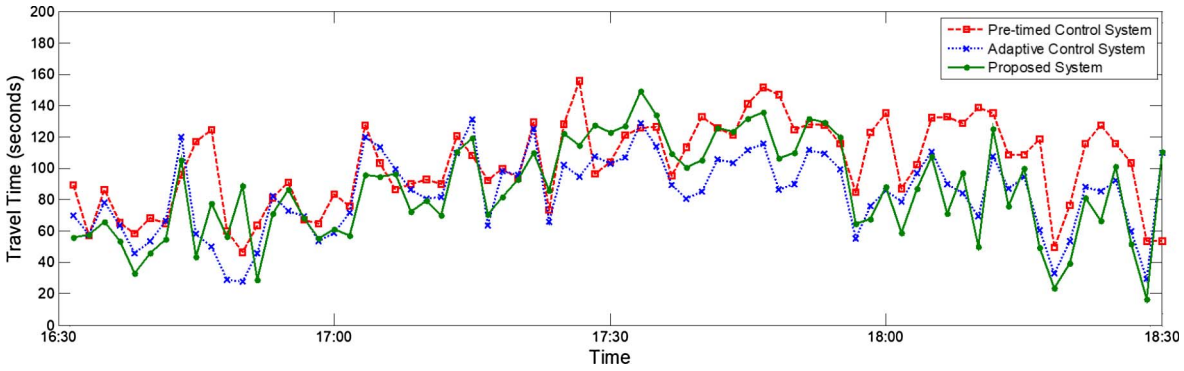

Fig. 12e. The time-dependent travel time along path 5.

Table 3
Network performance with different control systems.

Performance index	Pre-timed system	Adaptive system	Proposed system
Average number of stops	2.391	1.711 (−28.4%)	1.621 (−32.2%)
Average speed (km/h)	36.116	38.633 (+7.0%)	39.25 (+8.7%)
Average network delay (s)	89.065	73.77 (−13.7%)	68.209 (−19.6%)

the entire network with different MOEs, Table 3 summarizes the resulting average delays, average number of stops, and average speeds. Notably, the proposed system can produce the lowest network delay and the average number of stops, compared with the other two systems. Regarding the average speed, the proposed system can also yield significant improvement. However, one could also notice that the off-ramp priority control may result in some negative impacts to the local traffic. Based on the simulation results, it is noticeable that the adaptive system can outperform the pre-timed system on delay reduction while the proposed system can

significantly reduce the travel delay on freeway mainline with the slightly increase of delay on local traffic.

However, it shall be noted that the proposed system is mainly designed for preventing off-ramp queue spillover at the freeway interchange area, which requires the installation of both off-ramp dual-zone detectors and intersection loop detectors. For the implementation of regular arterial adaptive control, one shall only employ the control function described in Section 4.

7. Conclusions

This paper has illustrated an integrated real-time control system which includes three primary modules: off-ramp queue estimation, arterial adaptive signal control and freeway off-ramp priority control. Different from the conventional adaptive control systems, the proposed system will first estimate the queue length on the target off-ramp at the beginning of each signal cycle. Then, the priority control module will be activated to clear the queuing vehicles at the off-ramp when it predicts that potential freeway breakdown may incur due to off-ramp queue spillover. To evaluate the effectiveness of the proposed system, this study has conducted numerical studies on a real-world network, comprising both freeway mainline and local arterial, with a well-calibrated simulation platform. The experimental results reveal that the overall network performance has been significantly improved with the proposed control system. Further evaluation of the freeways travel time distribution has also demonstrated the effectiveness of the proposed system on preventing off-ramp queue spillover.

Further extensions along this line will be on contending with oversaturated traffic conditions where off-ramp queue spillover could not always be prevented. As such, a system wide control algorithm shall be implemented to improve the traffic operational efficiency over the entire corridor. Another future research issues associated with the proposed system is to integrate the off-ramp real-time control with freeway active control, such as variable speed limit operations and ramp metering controls.

Acknowledgments

The authors are grateful to the data provided by the National Chiao Tung University for its project sponsored by Taiwan Ministry of Communications and Transportation. This paper is partially supported by the National Science Foundation under Grant No. 1634641. Any opinions, findings, and conclusions or recommendations expressed in this material are those of the author and do not necessarily reflect the views of the National Science Foundation.

References

Cassidy, M.J., Anani, S.B., Haigwood, J.M., 2002. Study of freeway traffic near an off-ramp. Transp. Res. Part A: Policy Pract. 36 (6), 563–572.
Daganzo, C.F., Cassidy, M.J., Bertini, R.L., 1999. Possible explanations of phase transitions in highway traffic. Transp. Res. Part A: Policy Pract. 33 (5), 365–379.
Daganzo, C.F., Laval, J., Muñoz, J.C., 2002. Some ideas for freeway congestion mitigation with advanced technologies. Traffic Eng. Control 43 (10), 397–403.
Di, X., Zhang, X., Zhang, H.M., Liu, H.X., 2013. Application of pavement marker to avoid queue-jumping and traffic spillback at off-ramp of expressways. In: Transportation Research Board 92nd Annual Meeting, No. 13-3298.
Gartner, N.H., 1983. OPAC: a demand-responsive strategy for traffic signal control. In: Transportation Research Record 906, TRB, pp. 75–81.
Gartner, N.H., Stamatiadis, C., Tarnoff, P.J., 1995. Development of advanced traffic signal control strategies for ITS: a multilevel design. Transp. Res. Rec. 1494, 98–105.
Gartner, N.H., Pooran, F.J., Andrews, C.M., 2001. Implementation of the OPAC adaptive control strategy in a traffic signal network. In: Proceedings of the 2001 IEEE Intelligent Transportation Systems Conference. Oakland, California, pp. 195–200.
Gartner, N.H., Pooran, F.J., Andrews, C.M., 2002. Optimized policies for adaptive control strategy in real-time traffic adaptive control systems: implementation and field testing. Transp. Res. Rec.: J. Transp. Res. Board 1811 (1), 148–156.
Günther, G., Coeymans, J.E., Muñoz, J.C., Herrera, J.C., 2012. Mitigating freeway off-ramp congestion: a surface streets coordinated approach. Transp. Research Part C: Emerg. Technol. 20 (1), 112–125.
Henry, J.J., Farges, J.L., Tuffal, J., 1983. The PRODYN real time traffic algorithm. In: Proceedings of the Fourth IFAC-IFIP-IFORS Conference on Control in Transportation Systems, pp. 307–311.
Hunt, P.B., Robertson, D.I., Bretherton, R.D., Royle, M.C., 1982. The SCOOT on-line traffic signal optimisation technique. Traffic Eng. Control 23 (4).
Day, I., Ag, S., Whitelock, R., 1998. SCOOT-split, cycle & offset optimization technique. In: TRB Mid-Year Meeting and Adaptive Traffic Signal Control Workshop, vol. 7.
Jia, B., Jiang, R., Wu, Q.S., 2004. Traffic behavior near an off ramp in the cellular automaton traffic model. Phys. Rev. E 69 (5), 056105.
Li, Z., Chang, G.L., Natarajan, S., 2009. An integrated off-ramp control model for freeway traffic management. In: 15th World Congress on ITS. New York.
Lim, K., Kim, J.H., Shin, E., Kim, D.G., 2011. A signal control model integrating arterial intersections and freeway off-ramps. KSCE J. Civ. Eng. 15 (2), 385–394.
Little, J.D.C., Kelson, M.D., Gartner, N.H., 1981. MAXBAND: a program for setting signals on arteries and triangular networks. Transp. Res. Rec. 795, 40–46.
Lovell, D.J., 1997. Traffic Control on Metered Networks Without Route Choice (No. UCB-ITS-DS-97-3).
Lowrie, P.R., 1990. Scats, Sydney Co-ordinated Adaptive Traffic System: A Traffic Responsive Method of Controlling Urban Traffic.
Lu, X., Su, D., Spring, J., 2013. Coordination of Freeway Ramp Meters and Arterial Traffic Signals Field Operational Test. Report CA14-2223.
Mauro, V., Di Taranto, C., 1989. UTOPIA. In: CCCT'89 – AFCET Proceedings, Paris.
Messer, C.J., 1998. Simulation studies of traffic operations at oversaturated, closely spaced signalized intersections. Transp. Res. Rec.: J. Transp. Res. Board 1646 (1), 115–123.
Mirchandani, P., Head, L., 2001. A real-time traffic signal control system: architecture, algorithms, and analysis. Transp. Res. Part C 9 (6), 415–432.
Mirchandani, P.B., Head, K.L., Knyazyan, A., Wu, W., 2000. An approach towards the integration of bus priority, traffic adaptive signal control and bus information/scheduling system. Paper Presented at the 8th International Conference on Computer-Aided Scheduling of Public Transportation at Berlin, Germany.
Muñoz, J.C., Daganzo, C.F., 2002. The bottleneck mechanism of a freeway diverge. Transp. Res. Part A: Policy Pract. 36 (6), 483–505.
Newell, G.F., 1999. Delays caused by a queue at a freeway exit ramp. Transpo. Res. Part B: Methodol. 33 (5), 337–350.
Papageorgiou, M., Kotsialos, A., 2000. Freeway ramp metering: an overview. Proc. IEEE Intell. Transp. Syst. 228–239.
Pei, Y., Zhou, K., 2013. Off-ramp control near surface road. Res. J. Appl. Sci. Eng. Technol. 5 (8), 2612–2615.
Pooran, F.J., Lieu, H.C., 1994. Evaluation of system operating strategies for ramp metering and traffic signal coordination. In: Moving Toward Deployment. Proceedings of the IVHS America Annual Meeting, vol. 2.
Rudjanakanoknad, J., 2012. Capacity change mechanism of a diverge bottleneck. Transp. Res. Rec.: J. Transp. Res. Board 2278, 21–30.
Spiliopoulou, A., Kontorinaki, M., Papamichail, I., Papageorgiou, M., 2013. Real-time route diversion control at congested motorway off-ramp areas-Part I: user-optimum route guidance. In: 16th International IEEE Conference on Intelligent Transportation Systems-(ITSC), pp. 2119–2125.

Tian, Z.Z., 2007. Modeling and implementation of an integrated ramp metering-diamond interchange control system. J. Transp. Syst. Eng. Inform. Technol. 7 (1), 61–69.
Tian, Z.Z., Balke, K., Engelbrecht, R., Rilett, L., 2002. Integrated control strategies for surface street and freeway systems. Transp. Res. Rec.: J. Transp. Res. Board 1811 (1), 92–99.
Yang, X., Cheng, Y., Chang, G.L., 2014a. Real-Time Traffic Queue Length Estimation at the Freeway Off-ramp Using Dual-Zone Detectors. ITS World Congress, Detroit, Michigan.
Yang, X., Lu, Y., Chang, G.L., 2014b. Dynamic signal priority control strategy to mitigate off-ramp queue spillback to freeway mainline segment. Transp. Res. Rec.: J. Transp. Res. Board 2438, 1–11.
Yang, X., Cheng, Y., Chang, G.L., 2015a. A multi-path progression model for synchronization of arterial traffic signals. Transp. Res. Part C: Emerg. Technol. 53, 93–111.
Yang, X., Cheng, Y., Chang, G.L., 2015b. Integrating off-ramp spillback control with a decomposed arterial signal optimization model. Transp. Res. Rec.: J. Transp. Res. Board 2487, 112–121.